

This article was downloaded by:

On: 25 January 2011

Access details: *Access Details: Free Access*

Publisher *Taylor & Francis*

Informa Ltd Registered in England and Wales Registered Number: 1072954 Registered office: Mortimer House, 37-41 Mortimer Street, London W1T 3JH, UK



Liquid Crystals

Publication details, including instructions for authors and subscription information:

<http://www.informaworld.com/smpp/title~content=t713926090>

Physical effects of the surface elastic term K_{13} on weak anchoring nematic liquid crystal cells

Guan Ronghua Corresponding author^a; Huai Junxia^b; Yang Guochen^b

^a North China Electric Power University, Baoding 071003, PR China ^b Physics Institute of Hebei University of Technology, Tianjin 300130, PR China

Online publication date: 12 May 2010

To cite this Article Ronghua Corresponding author, Guan , Junxia, Huai and Guochen, Yang(2004) 'Physical effects of the surface elastic term K_{13} on weak anchoring nematic liquid crystal cells', *Liquid Crystals*, 31: 8, 1083 – 1091

To link to this Article: DOI: 10.1080/02678290410001703118

URL: <http://dx.doi.org/10.1080/02678290410001703118>

PLEASE SCROLL DOWN FOR ARTICLE

Full terms and conditions of use: <http://www.informaworld.com/terms-and-conditions-of-access.pdf>

This article may be used for research, teaching and private study purposes. Any substantial or systematic reproduction, re-distribution, re-selling, loan or sub-licensing, systematic supply or distribution in any form to anyone is expressly forbidden.

The publisher does not give any warranty express or implied or make any representation that the contents will be complete or accurate or up to date. The accuracy of any instructions, formulae and drug doses should be independently verified with primary sources. The publisher shall not be liable for any loss, actions, claims, proceedings, demand or costs or damages whatsoever or howsoever caused arising directly or indirectly in connection with or arising out of the use of this material.

Physical effects of the surface elastic term K_{13} on weak anchoring nematic liquid crystal cells

GUAN RONGHUA*

North China Electric Power University, Baoding 071003, PR China

HUAI JUNXIA and YANG GUOCHEN

Physics Institute of Hebei University of Technology, Tianjin 300130, PR China

(Received 18 November 2003; accepted 17 February 2004)

This paper aims at providing methods of checking whether the surface elastic term K_{13} exists or not, by studying the physical effects caused by K_{13} on weak anchoring planar NLC cells. We adopt the effective expression of K_{13} for an ideal surface according to Pergamenschik and Žumer, and obtain the following results. (1) $k = K_{13}^*/K_{11}$ can be determined by two threshold fields if both the Fréedericksz transitions at the threshold point are of second order. One threshold field corresponds to application of the external magnetic field perpendicular to the substrates; the other corresponds to the field parallel to the substrates. (2) The existence of the K_{13} term may change the property of the Fréedericksz transition, i.e. from first order to second order, or *vice versa*. (3) The various curves of relative optical retardation versus reduced magnetic field h for different k intersect at one point, and the slopes at the common point are sensitive to k . These results assist in the design of experiments to check the existence of K_{13} .

1. Introduction

According to Frank [1], the free energy density of a nematic liquid crystal caused by deformation of the director \mathbf{n} can be expressed as

$$f_F = \frac{1}{2}K_{11}(\nabla \cdot \mathbf{n})^2 + \frac{1}{2}K_{22}(\mathbf{n} \cdot \nabla \times \mathbf{n})^2 + \frac{1}{2}K_{33}(\mathbf{n} \times \nabla \times \mathbf{n})^2.$$

However, Nehring and Saupe [2] pointed out that there should be an additional two terms up to the order of $(\delta \mathbf{n})^2$ in f_F . These are

$$f_{24} = \frac{1}{2}(K_{22} + K_{24})\nabla \cdot [(\mathbf{n} \cdot \nabla)\mathbf{n} - \mathbf{n}(\nabla \cdot \mathbf{n})] \quad (1)$$

$$f_{13} = K_{13}\nabla \cdot (\mathbf{n}\nabla \cdot \mathbf{n}). \quad (2)$$

The total free energy density f_d becomes

$$f_d = f_F + f_{24} + f_{13}. \quad (3)$$

The contributions of the terms f_{24} and f_{13} to total free energy can eventually be written as surface energy; they are termed surface elastic energy.

In recent years there has been controversy over the existence of these two terms [3–12]. Many authors regard that they do not exist, because of the restrictions of elastic theory. However, Pergamenschik believes that

they do exist and regards this as one of the central problem of the physics of liquid crystals [13]. Whether these two terms exist or not should ultimately be examined experimentally. Recently, Stallinga *et al.* [14] have studied the effects of the K_{13} term on the electrically controlled birefringence (ECB) cell, but the conclusion is not satisfactory because of experimental inaccuracy. We believe this is because the considered effects are insensitive to the K_{13} term; some new physical effects, sensitive to the K_{13} term, must therefore be sought.

In this paper we seek new physical effects, sensitively dependent on K_{13} , by means of analytical methods and numerical calculation. In §2 we determine the Gibbs energy from which the differential equation and the boundary condition satisfying director \mathbf{n} are obtained. It should be emphasized that the interfaces should be considered as ideal, according to the continuum theory. Pergamenschik and Žumer [15] pointed out that both the density and scalar order parameter vary near the real surface layer. But this can eventually be changed into an ideal surface (the ideal surface refers to the density, and order parameters are uniform and equal to zero abruptly at the interface). The K_{13} term may be modified to an effective term K_{13}^* , which is called effective elastic constant. In §3 the threshold field of an

*Author for correspondence;
e-mail: ronghua_guan@sohu.com

LC cell under an external magnetic field will be considered; two cases are examined and calculated. One is splay transition (the external field perpendicular to the substrates), the other is twist transition (the external field parallel to the substrates). We obtain the formula $k = (K_{13}^*/K_{11})$ which can be used to judge whether the K_{13} term exists or not. In §4, we discuss the first order Fréedericksz transition, probably caused by the existence of the K_{13} term. Another method for testing the K_{13} term is also given. In §5, the relation between the relative optical retardation and K_{13} is considered, which can also be used to test for K_{13} .

2. The Gibbs free energy: equations and boundary condition

In a weak anchoring NLC cell, two substrates lie in the $z=0$ and $z=l$ planes, with the x axis in the lower substrate plane. Assuming the two substrates are identical, the easy direction \mathbf{e} in both substrates is the same and along the x axis. One external magnetic field \mathbf{H} is applied to the LC medium. Two cases may be considered. In the first, \mathbf{H} lies along the z axis and the director \mathbf{n} of the LC deflects from the x axis in the xz plane. Denoting the deflection angle by θ , the director \mathbf{n} can be expressed as $\mathbf{n} = (\cos \theta, 0, \sin \theta)$. In the second case, \mathbf{H} lies along the y axis and the director deflects from the x axis in the xy plane. Denoting the deflection angle by φ , the director \mathbf{n} can be expressed as $\mathbf{n} = (\cos \varphi, \sin \varphi, 0)$. Figures 1 and 2, respectively, illustrate the geometries of the two models.

Before writing out the Gibbs free energy, two points must be explained. One is the surface anchoring energy, the other is the elastic free energy. Rapini and Papoular have proposed a simple phenomenological expression for the anchoring energy per unit area [16]

$$g_s(\alpha) = \frac{1}{2} A_\alpha \sin^2 \alpha \tag{4}$$

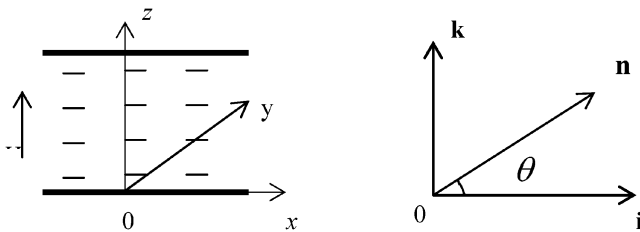


Figure 1. The mode of a planar alignment liquid crystal cell when applying an external magnetic field \mathbf{H} along the z axis. The director \mathbf{n} of the LC deflects from the x axis in the xz plane.

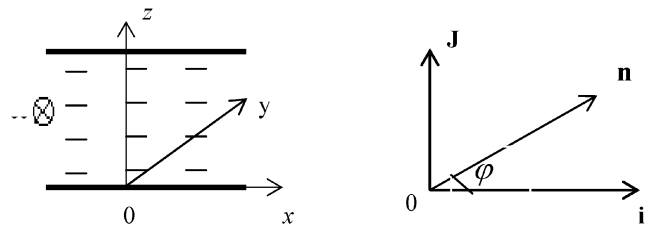


Figure 2. The mode of a planar alignment liquid crystal cell when applying an external magnetic field \mathbf{H} along the y axis. The director \mathbf{n} of the LC deflects from the x axis in the xy plane.

where α is the angle between the easy direction \mathbf{e} and the director \mathbf{n} of the NLC at the nematic–wall interface, and A_α is called the anchoring strength. This is the so-called RP formula. The RP formula describes many effects successfully in the presence of a surface. However, some results calculated from the RP formula do not agree well with experimental observations [17]. Many authors have introduced a new form of anchoring energy to replace the RP formula. If the lower order modification only is included, the new form can be expressed as [18, 19]

$$g_s(\alpha) = \frac{1}{2} A_\alpha \sin^2 \alpha (1 + \zeta \sin^2 \alpha) \tag{5}$$

where ζ is a modification constant. Formula (5) is a modification of (4) and has been accepted by most authors [14]. When the director distribution in a LC is calculated through continuum theory, the interfaces are assumed to be ideal. Hence formula (5) should be regarded as the effective surface density of anchoring energy.

On the other hand, if we adopt the ideal interface, constants K_{13} and K_{24} in equations (1)–(3) should be replaced by the effective elastic constants K_{13}^* and K_{24}^* in terms of Pergamanshchik’s theory [15].

For the first case of an external magnetic field \mathbf{H} along the z axis, the elastic free energy is

$$\begin{aligned} G_d &= \int f_d \, dv \\ &= S \left\{ \int_0^l dz \left[\left(\frac{1}{2} K_{11} \cos^2 \theta + \frac{1}{2} K_{33} \sin^2 \theta \right) \left(\frac{d\theta}{dz} \right)^2 \right. \right. \\ &\quad \left. \left. - K_{13}^* \cos \theta_0 \sin \theta_0 \frac{d\theta}{dz} \Big|_0 + K_{13}^* \cos \theta_l \sin \theta_l \frac{d\theta}{dz} \Big|_l \right] \right\} \tag{6} \end{aligned}$$

where S is the area of the substrate, and θ_0 and θ_l are the values of θ at $z=0$ and $z=l$, respectively. The total

free energy of the system can be written as

$$G = S \left\{ \int_0^l dz \left[\left(\frac{1}{2} K_{11} \cos^2 \theta + \frac{1}{2} K_{33} \sin^2 \theta \right) \left(\frac{d\theta}{dz} \right)^2 - \frac{1}{2} \chi_a \mathbf{H}^2 \sin^2 \theta \right] - K_{13}^* \cos \theta_0 \sin \theta_0 \frac{d\theta}{dz} \Big|_0 + K_{13}^* \cos \theta_l \sin \theta_l \frac{d\theta}{dz} \Big|_l + \frac{1}{2} A_\theta \sin^2 \theta_0 (1 + \zeta \sin^2 \theta_0) + \frac{1}{2} A_\theta \sin^2 \theta_l (1 + \zeta \sin^2 \theta_l) \right\}. \quad (7)$$

Applying the calculus of variations, equation (7) yields

$$(K_{11} \cos^2 \theta + K_{33} \sin^2 \theta) \frac{d^2 \theta}{dz^2} + \sin \theta \cos \theta (K_{33} - K_{11}) \frac{d\theta}{dz} + \chi_a \mathbf{H}^2 \sin \theta \cos \theta = 0 \quad (8)$$

with the boundary condition

$$\begin{aligned} & [(K_{11} + K_{13}^*) \cos^2 \theta_0 + (K_{33} - K_{13}^*) \sin^2 \theta_0] \theta'_0 \\ & = A_\theta \sin \theta_0 \cos \theta_0 (1 + 2\zeta \sin^2 \theta_0) - \frac{1}{2} K_{13}^* \sin 2\theta_0 \frac{d\theta'_0}{dz} \end{aligned} \quad (9)$$

where $\theta'_0 = \frac{d\theta}{dz} \Big|_{z=0}$, which should be a function of θ_0 . This boundary condition is also given in [14] and meets the requirement of [13].

For the second case of an external magnetic field \mathbf{H} along the y axis, the total free energy of the system can be written as

$$G = S \left\{ \int_0^l dz \left[\frac{1}{2} K_{22} \left(\frac{d\varphi}{dz} \right)^2 - \frac{1}{2} \chi_a H^2 \sin^2 \varphi \right] + \frac{1}{2} A_\varphi \sin^2 \varphi_0 (1 + \zeta \sin^2 \varphi_0) + \frac{1}{2} A_\varphi \sin^2 \varphi_l (1 + \zeta \sin^2 \varphi_l) \right\} \quad (10)$$

where φ_0 and φ_l are the values of φ at $z=0$ and $z=l$, respectively.

Applying the calculus of variations, equation (10) yields

$$K_{22} \frac{d^2 \varphi}{dz^2} + \chi_a H^2 \sin \varphi \cos \varphi = 0 \quad (11)$$

with the boundary condition

$$K_{22} \frac{d\varphi}{dz} \Big|_{z=0} = A_\varphi \sin \varphi_0 \cos \varphi_0 (1 + 2\zeta \sin^2 \varphi_0). \quad (12)$$

Comparing equations (7)–(9) with equations (10)–(12) we see that all equations in the second case of \mathbf{H} along the y axis can be obtained by letting $K_{11} = K_{33} = K_{22}$, $K_{13}^* = 0$, and by transforming θ to φ , A_θ to A_φ , in corresponding equations in the first case of \mathbf{H} along the z axis.

3. The fundamental equations, threshold field and the value of k

We first discuss the solutions of equation (8) with the boundary condition (9). Clearly there exist two trivial solutions: (i) $\theta \equiv 0$, the uniform solution, the corresponding LC state is called the uniform state; (ii) $\theta \equiv \pi/2$, the saturated solution, the corresponding LC state is called the saturated state. In addition, there is a

non-trivial solution satisfying $d\theta/dz \neq 0$, the corresponding LC state is called the disturbed state. From equation (8) we know that the disturbed state satisfies

$$\frac{d}{dz} [(K_{11} \cos^2 \theta + K_{33} \sin^2 \theta) \theta'^2 + \chi_a \mathbf{H}^2 \sin^2 \theta] = 0. \quad (13)$$

Assuming the director distribution is symmetric to the middle layer of the cell ($z = l/2$), when $z = l/2$, $\theta = \theta_m$ and $\frac{d\theta}{dz} \Big|_{z=l/2} = 0$. From equation (13) we obtain

$$(K_{11} \cos^2 \theta + K_{33} \sin^2 \theta) \theta'^2 = \chi_a \mathbf{H}^2 (\sin^2 \theta_m - \sin^2 \theta)$$

that is,

$$\frac{d\theta}{dz} = \left(\frac{\chi_a}{K_{11}} \right)^{\frac{1}{2}} \mathbf{H} \left(\frac{\sin^2 \theta_m - \sin^2 \theta}{1 + \gamma \sin^2 \theta} \right)^{\frac{1}{2}} \quad \left(\text{for } z < \frac{l}{2} \right) \quad (14)$$

where

$$\gamma = \frac{K_{33} - K_{11}}{K_{11}} \quad (15)$$

Integrating equation (14) results in

$$\frac{l}{2} \left(\frac{\chi_a}{K_{11}} \right)^{\frac{1}{2}} \mathbf{H} = \int_{\theta_0}^{\theta_m} \left(\frac{1 + \gamma \sin^2 \theta}{\sin^2 \theta_m - \sin^2 \theta} \right)^{\frac{1}{2}} d\theta. \quad (16)$$

In order to express the boundary condition of the disturbed solution definitely and make numerical calculation in the next sections, we make a variable transformation as follows. Letting

$$u = \sin^2 \theta_m, \quad v = \frac{\sin^2 \theta}{\sin^2 \theta_m}, \quad v_0 = \frac{\sin^2 \theta_0}{\sin^2 \theta_m} \quad (17)$$

and introducing the reduced field

$$h = \frac{\mathbf{H}}{\mathbf{H}_c^0} = \mathbf{H} / \left[\frac{\pi}{l} \left(\frac{K_{11}}{\chi_a} \right)^{\frac{1}{2}} \right] \quad (18)$$

then equation (16) can be expressed as

$$\frac{\pi}{2} h = \int_{v_0}^1 \frac{1}{2[v(1-v)]^{\frac{1}{2}}} \left(\frac{1 + \gamma uv}{1 - uv} \right)^{\frac{1}{2}} dv \quad (19)$$

Equation (19) is an integral equation in u and v_0 , and is transformed from the differential equation (14).

Now we also re-express the boundary condition with u and v_0 . From equation (14) we obtain

$$\theta'_0 = \frac{\pi}{l} h \left(\frac{u - uv_0}{1 + \gamma uv_0} \right)^{\frac{1}{2}} \quad (20)$$

and

$$\frac{d\theta'_0}{d\theta_0} = \frac{1}{2} \frac{\pi}{l} h \left(\frac{u - uv_0}{1 + \gamma uv_0} \right)^{\frac{1}{2}} \left[\frac{1}{u(1 + \gamma uv_0)} \frac{\partial u}{\partial \theta_0} - \frac{1 + \gamma u}{(1 - v_0)(1 + \gamma uv_0)} \frac{\partial v_0}{\partial \theta_0} \right]. \quad (21)$$

$\partial u / \partial \theta_0$ and $\partial v_0 / \partial \theta_0$ can be obtained from equations (19) and (17), respectively. Letting

$$I_1 = \int_{v_0}^1 \frac{1}{2[v(1-v)]^{\frac{1}{2}}} \left(\frac{1+\gamma uv}{1-uv} \right)^{\frac{1}{2}} dv \quad (22)$$

$$I_2 = \int_{v_0}^1 \frac{1}{2[v(1-v)]^{\frac{1}{2}}} \left(\frac{1+\gamma uv}{1-uv} \right)^{\frac{1}{2}} \cdot v dv \quad (23)$$

$$I_3 = \int_{v_0}^1 \frac{1}{2[v(1-v)]^{\frac{1}{2}}} \left(\frac{1+\gamma uv}{1-uv} \right)^{\frac{1}{2}} \cdot \frac{1}{(1+\gamma uv)(1-uv)} dv \quad (24)$$

the boundary condition (9) can be expressed as

$$I_1 \left\{ 1 + \frac{k}{1+k} \frac{v_0(1-uv_0)}{1+\gamma_1 uv_0} \left[\frac{1}{1-v_0} - \frac{1-Q}{Q} - \frac{\gamma u}{1+\gamma uv_0} \right] \right\} \\ = \alpha(1+2\zeta uv_0) \frac{1}{1+k} \frac{1+\gamma uv}{1+\gamma_1 uv_0} \left[\frac{v_0(1-uv_0)}{(1-v_0)(1+\gamma uv_0)} \right]^{\frac{1}{2}} \quad (25)$$

where

$$Q = v_0 + (1+\gamma)u \left[\frac{v_0(1-v_0)(1-uv_0)}{1+\gamma uv_0} \right]^{\frac{1}{2}} I_3 \quad (26)$$

$$\gamma_1 = \frac{K_{33} - K_{11} - 2K_{13}^*}{K_{11} + K_{13}^*} \quad (27)$$

$$k = \frac{K_{13}^*}{K_{11}}, \alpha = \frac{A_\theta \cdot l}{2K_{11}}$$

The derivation of the above equations is given in Appendix I.

From equations(19) and (22) we know

$$\frac{\pi}{2} h = I_1. \quad (28)$$

Defining the reduced free energy

$$g = \frac{lG}{2K_{11}S} \quad (29)$$

then the reduced free energies for the uniform state, saturated state and disturbed state are, respectively,

$$g_u = 0 \quad (30)$$

$$g_s = - \left(\frac{\pi}{2} h \right)^2 + \alpha(1+\zeta) \quad (31)$$

$$g_\theta = u \left\{ I_1^2 - 2I_1 I_2 - 2k \left[\frac{v_0(1-v_0)(1-uv_0)}{1+\gamma uv_0} \right]^{\frac{1}{2}} I_3 + \alpha v_0(1+\zeta uv_0) \right\}. \quad (32)$$

Equations(22)–(32) are the basic equations in this paper, and are suitable for the first case of **H** along the *z* axis. For the second case of **H** along the *y* axis, we let $K_{11} = K_{33} = K_{22}$, $K_{13}^* = 0$ and transform θ to φ and A_θ to A_φ .

We now discuss the threshold field. Suppose that the Fréedericksz transition is second order, temporarily.

Then

$$\frac{\pi}{2} h_{th} = I_1|_{u=0}$$

From equation (25)

$$I_1|_{u=0} = \frac{\alpha}{1+2k} \left(\frac{v_0}{1-v_0} \right)^{\frac{1}{2}}.$$

The threshold field for the first case of **H** along the *z* axis is denoted by $h_{th}^{(\perp)}$, and the following equation can be derived:

$$\cot\left(\frac{\pi}{2} h_{th}^{(\perp)}\right) = \left(\frac{1+2k}{\alpha}\right) \frac{\pi}{2} h_{th}^{(\perp)}. \quad (33)$$

For the second case of **H** along the *y* axis, the threshold field is denoted by $h_{th}^{(\parallel)}$. In equation (33), letting $K_{11} = K_{33} = K_{22}$, $K_{13}^* = 0$, i.e. $k = 0$, and

$$\alpha' = \frac{A_\varphi \cdot l}{2K_{22}} \quad (34)$$

we obtain

$$\cot\left(\frac{\pi}{2} h_{th}^{(\parallel)}\right) = \frac{1}{\alpha'} \frac{\pi}{2} h_{th}^{(\parallel)}. \quad (35)$$

Combining equation (33) with (35) gives

$$k = \frac{1}{2} \left[\frac{h_{th}^{(\parallel)} \cot\left(\frac{\pi h_{th}^{(\perp)}}{2}\right)}{h_{th}^{(\perp)} \cot\left(\frac{\pi h_{th}^{(\parallel)}}{2}\right)} \cdot \frac{\alpha}{\alpha'} - 1 \right]. \quad (36)$$

This is an important formula in our determination of *k*.

From equations(27) and (34), we obtain

$$\frac{\alpha}{\alpha'} = \frac{A_\theta K_{22}}{A_\varphi K_{11}}. \quad (37)$$

If the parameters K_{11} , K_{22} , χ_a , l , A_θ , A_φ are known and the threshold fields $h_{th}^{(\perp)}$ and $h_{th}^{(\parallel)}$ are measured by experiment, the value of *k* may be determined from equation(36). We can therefore judge whether K_{13} exists or not, based on the calculation results. Examples of curve $k - h_{th}^{(\perp)}$ are given in figure 3, showing that the difference between A_θ and A_φ affects the value of K_{13} , and that they are in proportion to each other. But this effect will fall with the increase of the threshold field $h_{th}^{(\perp)}$.

4. The first order Fréedericksz transition

In this section, we discuss the effects of the K_{13} term on the properties of the Fréedericksz transition. The reduced free energy must first be calculated. Equations(28) or (19), and (25), show the relationships of the three variables v_0 , h and u ; v_0 and h could be solved through these two equations for a given u . Therefore we take u as the state parameter (similar to an order parameter) of the LC, and express the reduced energy as a function of u . The values of u corresponding to

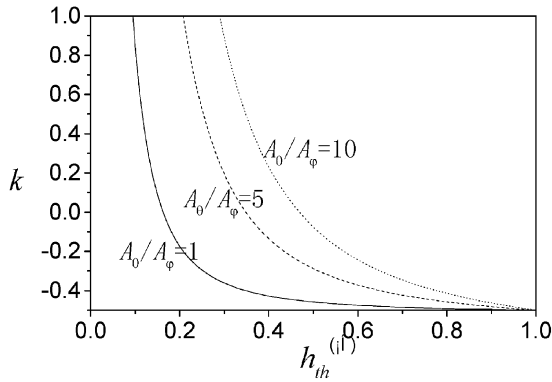


Figure 3. The reduced threshold field $h_{th}^{(l)}$ versus k for different A_0/A_ϕ with $K_{22}/K_{11} \approx 0.67$, $\alpha' = 0.1$.

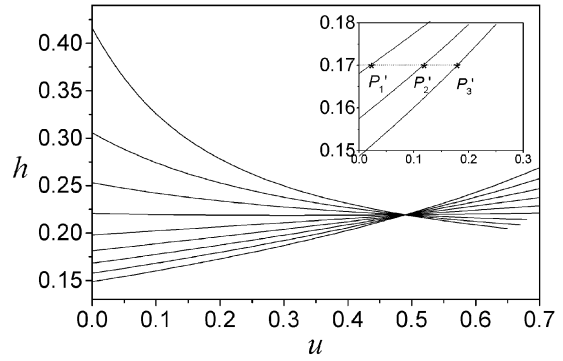


Figure 5. The function $h(u)$ for different values of k . As h is increased at $u=0$, the successive curves correspond to $k = -0.4, -0.3, -0.2, -0.1, 0, 0.1, 0.2, 0.3$ and 0.4 .

uniform state, saturated state and disturbed state are $u=0$, $u=1$ and $0 < u < 1$, respectively.

When u is known, the values of v_0 , h and g_θ may be determined from equations (22)–(32). Taking MBBA for example, the elastic constants $K_{11} = 5.8 \times 10^{-12}$ N, $K_{33}/K_{11} \approx 1.25$, $K_{22}/K_{11} \approx 0.67$ [20]; the anchoring energy strength $A_\theta \approx 2 \times 10^{-7}$ J m⁻² [21], the cell thickness $l = 5.8 \mu\text{m}$ [22] and $\zeta = 0.2$. The curves v_0-u , $h-u$ and $g_\theta-u$ obtained from the results of calculation are illustrated in figures 4–6, respectively.

The following results may be derived from these three figures:

- (1) The deviation of the director in the interfaces (denoted by $v_0 = \sin^2 \theta_0 / u$) is sensitive to K_{13}^* (denoted by $k = K_{13}^*/K_{11}$) for a given u . For example, in figure 4, the vertical line of $u=0.2$ intersects the curves for $k = -0.4, -0.3, -0.2$ at P_1, P_2, P_3 , with corresponding $v_0 = 0.859, 0.883, 0.899$, respectively.
- (2) The deviation of the director at the middle layer of the LC cell (denoted by $u = \sin^2 \theta_m$) is also

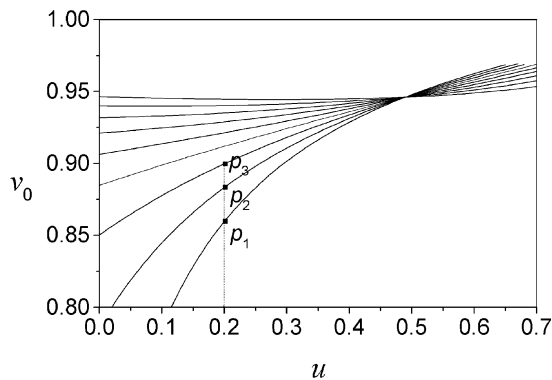


Figure 4. The function $v_0(u)$ for different values of k . As v_0 increases at $u=0$, the successive curves correspond to $k = -0.4, -0.3, -0.2, -0.1, 0, 0.1, 0.2, 0.3$ and 0.4 .

sensitive to K_{13}^* (denoted by $k = K_{13}^*/K_{11}$) for a given h . For example, in figure 5, the horizontal line of $h=0.17$ intersects the curves for $k=0.4, 0.3, 0.2$ at P'_1, P'_2, P'_3 , with corresponding $u=0.18, 0.12, 0.02$, respectively.

- (3) The reduced free energy of the disturbed state is also sensitive to the value of k , resulting in great differences in the curves of g_θ . From the expression of g_θ in equation (32) we see that there is a term directly relevant to k , apart from I_1, I_2 and v_0 , which are dependent on k . The curves for $k=0.1, 0, -0.1, -0.2$ are shown in figure 6 (curves for $k=0.2, 0.3, 0.4$ below $k=0.1$, and curves for $k=-0.3, -0.4$ above $k=-0.2$ are omitted).

The variation of free energy caused by the existence of the K_{13} term will change the property of the Fréedericksz transition. In figure 6, the curve $g_\theta-u$ for $k=0$ is tangential to the horizontal axis at $u=0$, then descends monotonically for $g_\theta < g_u$. The Fréedericksz transition thus occurs at the point $u=0$ and is second order. The curve $g_\theta-u$ for $k=-0.1$ is also tangential to the horizontal axis $g_\theta=0$ at $u=0$, but with increasing u

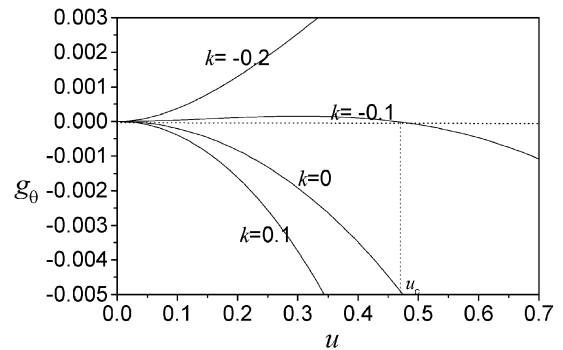


Figure 6. Order parameter u versus the reduced free energy g_θ of the disturbed state for different values of k .

it rises first, then falls and intersects the horizontal axis at $u_c=0.46$. Then $g_\theta \leq g_u$ only if $u \geq u_c$. Therefore is a Fréedericksz transition from uniform to disturbed state takes place at u_c and is first order. We therefore see that the existence of the K_{13}^* term may change the transition properties.

The K_{13}^* term may also give rise to bistability. Re-examining figure 6, the curve $g_\theta-u$ for $k=-0.2$ is tangential to the horizontal axis $g_\theta=0$ at $u=0$. But when $u>0$, the curve begins to rise monotonically with $g_\theta > g_u$. Hence no transition from uniform to disturbed state occurs. The saturation state is reached directly and the corresponding reduced field can be deduced with $g_u=g_s$. From equations (30) and (31), we obtain

$$h = \frac{2}{\pi} [\alpha(1+\zeta)]^{\frac{1}{2}} \tag{38}$$

In the course of the deviation of the director from uniform state ($u=0$) to saturated state ($u=1$), there is a deformation of the director and the free energy increases; this is equivalent to the existence of a barrier. As a result the uniform and saturated states can form a bistability.

The transitions from uniform to disturbed state and from uniform to saturated state are both of first order in the specific examples described above. We now give the condition for the first order transition in general cases. Adopting the method of Gouchen *et al.* [22], g_θ of equation (32) is expanded into a Taylor's series with respect to u at $u=0$:

$$g_\theta = Au + \frac{1}{2}Bu^2 + o(u^3) \tag{39}$$

The coefficients A, B can be calculated from equations (22)–(32) (See Appendix II). They are

$$A = 0$$

$$B = 2\alpha v_0^0 \left\{ \frac{1+\gamma}{8} \left[2v_0^0 - \frac{(1+2k)(1-v_0^0)+\alpha}{(1+2k)(1-v_0^0)} \right] - \zeta v_0^0 \right. \tag{40}$$

$$\left. - \frac{3(1+\gamma)kv_0}{2(1+2k)} - \frac{(1+\gamma)k}{4(1+2k)^2(1-v_0)} [(1+2k)(1-v_0^0)+\alpha] \right\}$$

where v_0^0 is the value of v_0 at $u=0$. Because the condition for the first order transition is $g_\theta \geq 0$, it requires

$$B \geq 0 \tag{41}$$

Equations (40) and (41) indicate that the first order transition taking place in the LC cell is determined by

four parameters: α, ζ, γ and k . The first three are decided by the construction of LC cell and the Frank elastic constants K_{11}, K_{33} of the materials; the last one is determined by K_{13}^* . The sign of k and its absolute value are crucial for the transition properties. We can therefore judge whether K_{13}^* is equal to zero or not according to the transition properties. As a specific example we take $\gamma=0.25$ and draw the curve $B=0$ in a $\alpha-\zeta$ plot based on equations (40) and (41). The curve is the line of demarcation of the first and the second order transitions; see figure 7.

There are three curves in figure 7, corresponding to $k=0, k=0.1$ and $k=-0.1$. The first and second transition areas do not coincide. Looking at the shaded area in figure 7 for example, when $k=0$ it belongs to the second order transition area, but for $k=-0.1$ it is in the first order transition area. We chose α and ζ in the shaded, are a such that $\alpha=1.0, \zeta=-0.5$. If the value of k is really equal to zero, the transition will be second order, but for $k=-0.1$ it will be first order. That is to say, if a first order transition is observed, then $k \neq 0$, i.e. K_{13}^* has a non-zero value.

5. Optical retardation, intersection and slope

The optical retardation has previously been given for the first case of \mathbf{H} along the z axis by [23]

$$\delta = \frac{4\pi}{\lambda} \int_{\theta_0}^{\theta_m} \left(\frac{n_0 n_e}{(n_e^2 \sin^2 \theta(z) + n_0^2 \cos^2 \theta(z))^{\frac{1}{2}}} - n_0 \right) \left(\frac{dz}{d\theta} \right) d\theta \tag{42}$$

where λ is the wavelength of the light and n_0 and n_e are the ordinary and extraordinary indices of refraction, respectively. Substituting equation (14) into (42) and transforming it to a function about u, v and v_0 , the

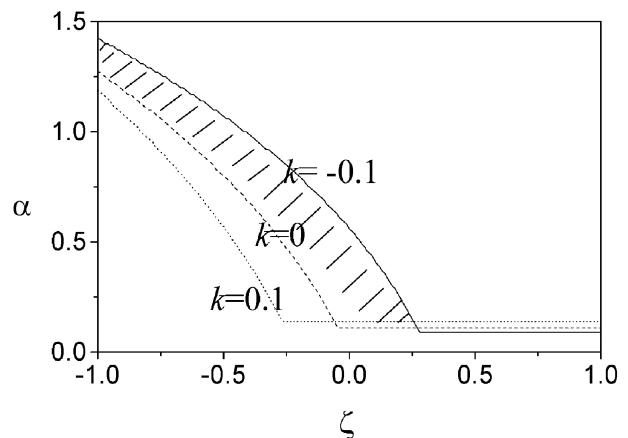


Figure 7. Parameter ζ versus the reduced anchoring strength α for different values of k with $\gamma=0.25$. The area above each curve belongs to the second order transition area; below is the first order transition area.

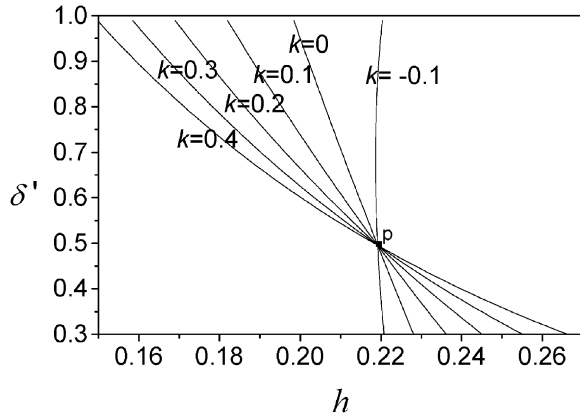


Figure 8. The reduced field h versus the relative optical retardation δ' for different values of k , taking the same material parameters as used in figures 2 and 3.

relative optical retardation can be expressed as

$$\delta' = \frac{\delta}{\delta_0} = \frac{n_0}{2I_1(n_e - n_0)} \int_{v_0}^1 \left[\frac{1}{(1 - \Gamma + \Gamma uv)^{\frac{1}{2}}} - 1 \right] \left[\frac{1 + \gamma uv}{v(1-v)(1-uv)} \right]^{\frac{1}{2}} dv \quad (43)$$

where $\Gamma = (n_e^2 - n_0^2)/n_e^2$; $\delta_0 = 2\pi l(n_e - n_0)/\lambda$ is the optical retardation for zero \mathbf{H} or if the value of \mathbf{H} is below the threshold field.

The relationship between δ' and h may be obtained by combining equations (25) and (28). In the preceding section we took a set of parameters to give curves of $v_0 - u$ and $h - u$. The same parameters are used to draw the curves of $\delta' - h$. Taking $\lambda = 632.8 \text{ nm}$, $n_e = 1.573$ and $n_0 = 1.477$ [14], the results shown in figure 8 may be derived. Because, when $k = -0.2, -0.3, -0.4$, the Fréedericksz transition is first order and the director becomes directly saturated at $u = 0$, these curves are not shown in figure 8.

Figures 8, 4 and 5 are particularly noteworthy: there is a common point for each curve for different values of k (including $k = 0$). But their slopes are different at the point of intersection and vary monotonically with k . In figure 8 for the cases of $k > 0$, the slopes are negative and their absolute values decrease with the increase of k .

Although figure 8 only reflects a particular example, it provides useful information: whether or not K_{13}^* is equal to zero could be concluded from the slopes at the intersection of the $\delta' - h$ curves. The common point u_p is

determined by the following two equations

$$I_1 = \alpha(1 + 2\zeta uv_0) \left(\frac{v_0}{1 - v_0} \right)^{\frac{1}{2}} \left(\frac{1 - uv_0}{1 + \gamma uv_0} \right)^{\frac{1}{2}} \quad (44)$$

$$Q = \frac{v_0(1 - uv_0)(1 + \gamma uv_0)}{(2v_0 - 1) + (uv_0)(2 - 3v_0 + \gamma v_0) + (uv_0)^2 \gamma (1 - 2v_0)} \quad (45)$$

Equation (44) is the boundary condition for the case of $k = 0$, and equation (45) is the condition that is unconcerned with the value of k . They both come from equation (25). Furthermore the slopes at $u = u_p$ in figure for $\delta' - h$ can be calculated from

$$\frac{d\delta}{dh} \Big|_{u=u_p} = \frac{d\delta}{du} \Big|_{u=u_p} / \frac{dh}{du} \Big|_{u=u_p} \quad (46)$$

We have attempted to calculate the final results of equation (46) using the first order derivatives of equations (43) and (19). But the process is so complicated that it will not be set out here. Taking figure 8 for example, the slopes of each curve are tabulated for the intersection $u_p = 0.4898$, $v_{0p} = 0.9461$, $h_p = 0.2192$, $\delta'_p = 0.4954$. It can be seen from the table that the slope is sensitive to the value of k ; and whether or not k is zero can therefore be judged.

6. Discussion

We have discussed the physical effects caused by the surface terms of free energy. The surface terms include three parts: the K_{13} term, the K_{24} term and the anchoring term. But the question is how to separate these three terms; in this paper we propose the following methods:

- (1) By adopting a liquid crystal cell with two parallel substrates, the $(\mathbf{n} \cdot \nabla \mathbf{n} \cdot \mathbf{n})$ term in equation (1) is definitely perpendicular to the normal of the substrates; so the K_{24} term disappears automatically.
- (2) Two experiments are carried out on the same LC cell. One is with the external field \mathbf{H} perpendicular to the substrates and the other uses the parallel \mathbf{H} condition. For the parallel case the K_{13} term also vanishes automatically, therefore only the anchoring energy is left in the surface terms. We use this case to determine

Table. Parameter slopes for different values of k .

Slope	$k = -0.4$	$k = -0.3$	$k = -0.2$	$k = -0.1$	$k = 0$	$k = 0.1$	$k = 0.2$	$k = 0.3$	$k = 0.4$
$\frac{dv_0}{du} \Big _{u_p}$	0.1694	0.1498	0.1304	0.1111	0.0921	0.0732	0.0545	0.0359	0.0175
$\frac{dh}{du} \Big _{u_p}$	-0.1128	-0.073	-0.0335	0.0056	0.0444	0.0828	0.1208	0.1585	0.1958
$\frac{d\delta'}{du} \Big _{u_p}$	-1.011	-1.0079	-1.0047	-1.0015	-0.9984	-0.9953	-0.9927	-0.9892	-0.9862
$\frac{d\delta'}{dh} \Big _{u_p}$	8.9634	13.8132	29.9964	-178.425	-22.507	-12.028	-8.2145	-6.2417	-5.036

the anchoring energy; then it is possible to test the K_{13} term based on the above.

In this paper we propose three different solutions to verify the existence or otherwise of the K_{13} term. The first is to determine two threshold fields with the external magnetic field \mathbf{H} perpendicular or parallel to the substrates; the second solution is to observe the properties of the Fréedericksz transition; the third is to determine the slopes at the intersection for the curves of reduced field h versus optical retardation δ' . Among these three solutions the first is easy to execute; in the second, it is necessary to consider the physical effects caused by the first order transition for precise discrimination; the third must be coordinated with theory. But whether the K_{13} term exists or not is a basic question. So we need to use different experimental methods from various points of view for thorough testing.

APPENDIX I

The derivation of equation (25)

The derivative of v_0 in equation (17) with respect to θ_0 can be written as

$$\begin{aligned} \frac{\partial v_0}{\partial \theta_0} &= \frac{2 \sin \theta_0 \cos \theta_0}{\sin^2 \theta_m} - \frac{2 \sin^2 \theta_0 \cos \theta_m}{\sin^3 \theta_m} \frac{\partial \theta_m}{\partial \theta_0} \\ &= 2 \left[\frac{v_0(1-uv_0)}{u} \right]^{\frac{1}{2}} - \frac{v_0}{u} \cdot \frac{\partial u}{\partial \theta_0}. \end{aligned} \tag{A1}$$

For a given h , taking the derivative for the two sides of equation (19) with respect to θ_0 yields

$$\begin{aligned} & - \frac{1}{2[v_0(1-v_0)]^{\frac{1}{2}}} \left(\frac{1+\gamma uv_0}{1-uv_0} \right)^{\frac{1}{2}} \frac{\partial v_0}{\partial \theta_0} \\ & + \int_{v_0}^1 \frac{\partial}{\partial \theta_0} \left\{ \frac{1}{2[v(1-v)]^{\frac{1}{2}}} \left(\frac{1+\gamma uv}{1-uv} \right)^{\frac{1}{2}} \right\} = 0. \end{aligned} \tag{A2}$$

Obtaining the derivative of the integrand in equation (A2) with respect to θ_0 ,

$$\frac{\partial}{\partial \theta_0} \left(\frac{1+\gamma uv}{1-uv} \right)^{\frac{1}{2}} = \frac{1+\gamma}{2} \frac{v}{(1-uv)[(1+\gamma uv)(1-uv)]^{\frac{1}{2}}} \cdot \frac{\partial u}{\partial \theta_0}. \tag{A3}$$

Substituting equation (A3) into (A2) and using (A1), we have

$$\frac{\partial u}{\partial \theta_0} = \frac{2[uv_0(1-uv_0)]^{\frac{1}{2}}}{Q} \tag{A4}$$

where Q is defined by equation (26); therefore (21) can

take the form

$$\frac{d\theta'_0}{d\theta_0} = \frac{1}{2} \frac{\pi}{l} h \left[\frac{u(1-v_0)}{1+\gamma uv_0} \right]^{\frac{1}{2}} \left\{ \frac{1}{u(1-v_0)} \left[\frac{\partial u}{\partial \theta_0} - 2(uv_0(1-uv_0))^{\frac{1}{2}} \right] - \frac{\gamma}{1+\gamma uv_0} \right\} \tag{A5}$$

Substituting equation (A4) into (A5), yields

$$\frac{d\theta'_0}{d\theta_0} = \frac{\pi}{l} h \left[\frac{u(1-v_0)}{1+\gamma uv_0} \right]^{\frac{1}{2}} \left\{ \left[\frac{v_0(1-uv_0)}{u(1-v_0)} \right]^{\frac{1}{2}} \frac{1-Q}{Q} - \frac{\gamma}{1+\gamma uv_0} \right\}. \tag{A6}$$

We also can express equation (9) with u , v_0 and define the reduced anchoring energy strength α and k as with equation (25). Substituting equations (20) and (A6) into (9), yields

$$\begin{aligned} I_1 &= \left\{ \alpha(1+2\zeta uv_0) - ku[v_0(1-v_0)]^{\frac{1}{2}} \left(\frac{1-uv_0}{1+\gamma uv_0} \right)^{\frac{1}{2}} I_1 \left[\frac{1}{u(1-v_0)} \frac{1-Q}{Q} - \frac{\gamma}{1+\gamma uv_0} \right] \right\} \\ & \quad \frac{1}{1+k} \frac{1+\gamma uv_0}{1+\gamma uv_0} \left[\frac{v_0(1-uv_0)}{(1-v_0)(1+\gamma uv_0)} \right]^{\frac{1}{2}} \end{aligned} \tag{A7}$$

Rearrangement of equation (A7) gives equation (25).

APPENDIX II

Derivation of the condition of the first order transition

The expression of the reduced free energy for the disturbed state is defined in equation (32).

The values of I_1 , I_2 and the first order derivatives of I_1 , I_2 with respect to u at $u=0$ can be expressed as:

$$I_1|_{u=0} = \arccos \sqrt{v} \tag{A8}$$

$$\begin{aligned} I'_1|_{u=0} &= - \frac{1}{2[v_0(1-v_0)]^{\frac{1}{2}}} \frac{dv_0}{du} \Big|_{u=0} \\ & + \frac{1+\gamma}{4} \left\{ [v_0(1-v_0)]^{\frac{1}{2}} + \arccos \sqrt{v} \right\} \end{aligned} \tag{A9}$$

$$I_2|_{u=0} = \frac{1}{2} \left\{ [v_0(1-v_0)]^{\frac{1}{2}} + \arccos \sqrt{v_0} \right\} \tag{A10}$$

$$\begin{aligned} I'_2|_{u=0} &= - \frac{1}{2} \left(\frac{v_0}{1-v_0} \right)^{\frac{1}{2}} \frac{dv_0}{du} \Big|_{u=0} + \frac{3}{16} (1+\gamma) \\ & \quad \left\{ [v_0(1-v_0)]^{\frac{1}{2}} \left(\frac{2}{3} v_0 + 1 \right) + \arccos \sqrt{v_0} \right\}. \end{aligned} \tag{A11}$$

The first order derivative of the reduced free energy is

$$\begin{aligned} A = \frac{dg}{du} \Big|_{u=0} &= \left\{ I_1^2 - 2I_1I_2 - 2k \left[\frac{v_0(1-v_0)(1-uv_0)}{1+\gamma uv_0} \right]^{\frac{1}{2}} I_1 \right. \\ & \quad \left. + \alpha v_0(1+\zeta uv_0) \right\} \Big|_{u=0}. \end{aligned} \tag{A12}$$

Substituting equation (A8) and (A10) into (A12), we obtain

$$A = \alpha v_0 - (1+2k)[v_0(1-v_0)]^{\frac{1}{2}} \arccos \sqrt{v_0}. \tag{A13}$$

The boundary condition (25) at $u=0$ is

$$\arccos \sqrt{v_0} = \frac{\alpha}{1+2k} \left(\frac{v_0}{1-v_0} \right)^{\frac{1}{2}} \quad (\text{A14})$$

Substituting equation (A14) into (A13) yields

$$A=0.$$

The second order derivative of the reduced free energy has the form

$$B = \frac{d^2 g_\theta}{du^2} \Big|_{u=0} = 2 \{ I_1^2 - 2I_1 I_2 - 2k \left[\frac{v_0(1-v_0)(1-uv_0)}{1+\gamma uv_0} \right]^{\frac{1}{2}} I_1 + \alpha v_0(1+\zeta uv_0) \} \Big|_{u=0}. \quad (\text{A15})$$

Substituting equation (A8)–(A11) into (A15), one has

$$B = \left[(1+2k+2\alpha) - \frac{\alpha}{1-v_0} + \frac{2\alpha v_0}{1-v_0} \frac{dv_0}{du} - \frac{1+\gamma}{2} (1+2k)v_0(1-v_0) - \frac{3}{4}(1+\gamma) \left\{ [v_0(1-v_0)]^{\frac{1}{2}} \left(\frac{2}{3}v_0 + 1 \right) \right\} \arccos \sqrt{v_0} + 2\alpha \zeta v_0^2 + (1+\gamma)k \left\{ [v_0(1-v_0)]^{\frac{1}{2}} (2v_0 - 1) \right\} \arccos \sqrt{v_0} - \frac{1+\gamma}{4} (\arccos \sqrt{v_0})^2 \right] \quad (\text{A16})$$

Taking the first order derivative of equation (25) with respect to u at $u=0$, we obtain the expression for dv_0/du at $u=0$

$$\frac{dv_0}{du} \Big|_{u=0} = \left\{ \frac{1+\gamma}{2} + \alpha \left[(1+\gamma) - 4\zeta - \frac{6k(1+\gamma)}{1+2k} \right] \frac{v_0}{(1+2k)(1-v_0) + \alpha} - \frac{1+\gamma}{1+2k} \frac{\alpha k}{(1+2k)(1-v_0)} \right\} v_0(1-v_0). \quad (\text{A17})$$

Substituting equation (A17) into (A16), gives equation (40).

References

- [1] FRANK, F. C., 1958, *Discuss. Faraday Soc.*, **25**, 19.
- [2] NEHRING, J., and SAUPE, A., 1971, *J. chem. Phys.*, **54**, 337.
- [3] BARBERO, G., and OLDANO, C., 1985, *Nuovo Cimento D*, **6**, 479.
- [4] BARBERO, G., GABBASOVA, Z., and OSIPOV, M. A., 1991, *J. Phys. II*, **1**, 691.
- [5] PERGAMENSHCHIK, V. M., 1993, *Phys. Rev. E*, **48**, 1254.
- [6] LAVRETOVICH, O. D., and PERGAMENSHCHIK, V. M., 1994, *Phys. Rev. Lett.*, **73**, 979.
- [7] FAETTI, S., 1994, *Phys. Rev. E* **49**, 5332; FAETTI, S., 1994, *Phys. Rev. E*, **49**, 4192.
- [8] FAETTI, S., and RICCARDI, M., 1995, *J. Phys. II*, **5**, 1165.
- [9] PONTI, S., 1995, *Phys. Lett. A*, **200**, 165.
- [10] STALLINGA, S., and VERTOGEN, G., 1996, *Phys. Rev. E*, **53**, 1692.
- [11] BARBERO, G., and FAETTI, S., 1996, *Phys. Rev. E*, **54**, 5866(c).
- [12] YOKOYAMA, H., 1997, *Phys. Rev. E*, **55**, 2938.
- [13] PERGAMENSHCHIK, V. M., 1998, *Phys. Rev. E*, **58**, R16.
- [14] STALLINGA, S., VAN HAAREN, J. A. M. M., and VAN DEN EERENBEEMD, J. M. A., 1996, *Phys. Rev. E*, **53**, 1701.
- [15] PERGAMENSHCHIK, V. M., and ŽUMER, S., 1999, *Phys. Rev. E*, **59**, R2531.
- [16] RAPINI, A., and PAPOULAR, M., 1969, *J. Phys. (Paris) Colloq.*, **30**, C4–54.
- [17] SONIN, A., 1995, *The Surface Physics of Liquid Crystals* (Gordon and Breach).
- [18] YOKOYAMA, H., and VAN SPRANG, H. A., 1985, *J. appl. Phys.*, **57**, 4520.
- [19] YANG, K. H., and ROSENBLATT, CH., 1983, *Appl. Phys. Lett.*, **41**, 438.
- [20] JÉRÔME, B., 1991, *Rep. Prog. Phys.*, **54**, 391.
- [21] YA, T., MARUSIY, YU., REZNIKOV, A., and RESHETNYAK, V. YU., 1987, *Mol. Cryst. liq. Cryst.*, **152**, 495.
- [22] GUOCHEN, Y., JIANRU, S., and YING, L., 2000, *Liq. Cryst.*, **27**, 875.
- [23] BLINOV, L. M., and CHIGRINOV, V. G., 1994, *Electro-optic Effects in Liquid Crystal Materials* (New York: Springer-Verlag).